



HAL
open science

Small angle neutron scattering (SANS) study of γ' precipitates in single crystals of AM1 superalloy

D. Bellet, P. Bastie, A. Royer, J. Lajzerowicz, J. Legrand, R. Bonnet

► To cite this version:

D. Bellet, P. Bastie, A. Royer, J. Lajzerowicz, J. Legrand, et al.. Small angle neutron scattering (SANS) study of γ' precipitates in single crystals of AM1 superalloy. Journal de Physique I, 1992, 2 (6), pp.1097-1112. 10.1051/jp1:1992199 . jpa-00246591

HAL Id: jpa-00246591

<https://hal.science/jpa-00246591>

Submitted on 4 Feb 2008

HAL is a multi-disciplinary open access archive for the deposit and dissemination of scientific research documents, whether they are published or not. The documents may come from teaching and research institutions in France or abroad, or from public or private research centers.

L'archive ouverte pluridisciplinaire **HAL**, est destinée au dépôt et à la diffusion de documents scientifiques de niveau recherche, publiés ou non, émanant des établissements d'enseignement et de recherche français ou étrangers, des laboratoires publics ou privés.

Classification

Physics Abstracts

81.40G — 61.12E — 61.16D

Small angle neutron scattering (SANS) study of γ' precipitates in single crystals of AM1 superalloy

D. Bellet ⁽¹⁾, P. Bastie ⁽¹⁾, A. Royer ⁽¹⁾, J. Lajzerowicz ⁽¹⁾, J. F. Legrand ⁽²⁾
and R. Bonnet ⁽³⁾

⁽¹⁾ Laboratoire de Spectrométrie Physique (*), Université Joseph Fourier Grenoble I, BP 87, 38402 Saint Martin d'Hères Cedex, France

⁽²⁾ Institut Laue Langevin BP 156X, 38042 Grenoble Cedex, France

⁽³⁾ Laboratoire de Thermodynamique et Physico-Chimie Métallurgiques (**), ENSEEG, BP 75, 38402 Saint Martin d'Hères Cedex, France

(Received 31 January 1992, accepted 17 March 1992)

Abstract. — The morphology of γ' precipitates of AM1 single crystal superalloys has been studied by small neutron scattering (SANS), and electron microscopy. Due to the single crystal nature of the samples, the SANS patterns are anisotropic and exhibit a fourfold symmetry corresponding both to the shape and to the spatial arrangement of the precipitates in a (001) plane. Measurements for other sample orientations have allowed us to improve the analysis of the shape of the precipitates. After creep deformation along the $\langle 001 \rangle$ axis, a twofold symmetry corresponding to the « rafting » of the γ' precipitates is observed in the (010) plane. The main effect of heat treatments at 1 050 °C, commonly used for industrial applications, is the coarsening of the precipitates. From the displacement of the correlation peaks towards smaller angles, we deduce an average centre-to-centre spacing between the precipitates which increases with the annealing time from 0.3 μm to 0.6 μm according to the Lifshitz, Slyosov, Wagner behaviour. The results are compared to electron microscopy measurements, performed on the same samples.

1. Introduction.

Constant efforts have been devoted to study and develop new materials which could improve the performances of aircraft engines. Nickel based superalloys are used in high temperature parts such as turbine blades. Indeed, these superalloys exhibit exceptional mechanical characteristics at high temperatures. Their yield stress increases with temperature [1] and they can be used in corrosive environments [2]. Such properties and industrial interests have driven a number of basic studies of these materials.

A key feature in the mechanical properties of the superalloys is their diphasic nature : they include precipitates which hinder the gliding of dislocations [3, 4]. The matrix is a disordered

(*) Associé au CNRS, URA n 08.

(**) Associé au CNRS, URA n 29.

f.c.c. alloy (γ phase), in which grow ordered γ' precipitates with $L1_2$ structure. The morphology of the γ' precipitates (shape, size and spatial arrangement) is a parameter which plays an important role in the mechanical properties of the superalloys at high temperatures [5-8]. In the recent superalloys the volume fraction of the ordered phase is rather large at room temperature (70 %) and it remains almost constant up to 1 000 °C [9]. Moreover, the manufacture of superalloy single-crystal turbine blades has allowed to achieve substantial improvement of creep and fatigue properties [6].

The morphology of the γ' precipitates can be modified by heat treatments. A study of the CMSX-2 superalloy has shown that a microstructure with a regular arrangement of cubic γ' precipitates (with edge size of 0.45 μm) corresponds to an optimal creep resistance. These observations have led to define the standard ONERA heat treatment (3 hours at 1 300 °C followed by 16 hours at 1 050 °C and 48 hours at 850 °C) which is commonly used as reference [5]. But it has also been reported that the size of the precipitates is not the only relevant parameter to describe the creep behaviour at high temperatures : their shape and their spatial arrangement should be also taken into account [9]. When the CMSX-2 superalloy is submitted to annealing at 1 000 °C during a very long time (28 days), the morphology of the γ' precipitates evolves towards a « bamboo structure » [10]. During tensile deformations of the CMSX-2 or AM1 superalloys at high temperatures (near 1 000 °C), the γ' precipitates coarsen into the form of platelets perpendicular to the stress axis [4, 9]. The transformation from cubic into platelet-shaped precipitates (« rafting ») leads to a much lower creeping rate and therefore to a longer lifetime before rupture at high temperatures [8].

Understanding the origin of the evolution of γ' precipitates' morphology *versus* annealing treatment or under stress remains an important problem. Its study is difficult because of the large number of parameters which can influence the morphology of the γ' precipitates [11]. Among these parameters, the mismatch between the lattice parameters, the elastic energy of the interface and the chemical heterogeneities play an important role but their experimental observations are rather difficult and some discrepancies about their values are found in the literature. See for instance [10, 12] and [13] for the lattice mismatch.

The present study concerns the AM1 superalloy [14] which belongs to the same class of superalloys as the prototype CMSX-2. It is based on the use of small angle neutron scattering (SANS) : a non-destructive and bulk sensitive technique [15, 16]. Preliminary results on single crystalline samples have shown that SANS experiments permit an analysis of the shape, the size and the arrangement of the γ' precipitates [17, 18]. In the study reported here, we have investigated these morphological features as a function of the thermal history of the specimens.

The sample preparation and the experimental procedure are described in section 2. The small-angle scattering results are reported in section 3 ; they show interesting features related to the single crystal character of the materials. Finally the results are discussed in section 4 and compared to observations using electron microscopy.

2. Material and experimental procedure.

The chemical composition of the AM1 superalloy is shown in table I ; the density is equal to 8.6 and the melting point is close to 1 350 °C. The single crystal has been grown at the SNECMA foundry by the directional solidification method. It has a cylindrical shape (13 mm of diameter), with the growth axis parallel to the $\langle 001 \rangle$ crystallographic direction. Samples were cut by spark-erosion into small discs of about 1 mm thickness perpendicular to the $\langle 001 \rangle$ direction.

A preliminary annealing has been performed in order to homogenize the chemical composition of the alloy ($T = 1\,300$ °C for 45 minutes). Subsequent quenching in the air

Table I. — *Chemical composition of the AM1 superalloy (wt %).*

Ni	Co	Cr	Mo	W	Al	Ti	Ta
Balance	6.5	7.5	2.0	5.5	5.3	1.2	8.0

produces relatively homogeneous and small size γ' precipitates. After cutting, each disc was submitted to annealing at $T = 1\,050\text{ }^\circ\text{C}$ for times from 0 to 480 hours. This thermal treatment was performed in air and quenching was realized by pulling out the samples from the oven to the air at room temperature. A mechanical polishing of disc surfaces was performed after heat treatment in order to avoid spurious scattering from the oxidized surface.

Due to the large size of the precipitates after annealing (about $0.5\ \mu\text{m}$), small values of $q = 4\pi(\sin\theta)/\lambda$ have to be reached for the measurements (2θ is the scattering angle). So the experiments were performed using the small-angle scattering instrument D11 at the ILL [19, 20]. A wavelength of $10\ \text{\AA}$ (with 9% FWHM) was selected and the following configurations were chosen for the sample-detector distance D and the collimation length of the beam C :

i) $D = 35\ \text{m}$, $C = 40\ \text{m}$ in order to explore the range $6 \times 10^{-4} < q < 6 \times 10^{-3}\ \text{\AA}^{-1}$, hereafter called *small- q range*.

ii) $D = 15\ \text{m}$, $C = 20\ \text{m}$ $1.5 \times 10^{-3} < q < 1.5 \times 10^{-2}\ \text{\AA}^{-1}$ or $D = 10\ \text{m}$, $C = 10\ \text{m}$ $2 \times 10^{-3} < q < 2 \times 10^{-2}\ \text{\AA}^{-1}$, hereafter called *large- q range*.

The experiments reported here were performed at room temperature. Considering the chemical composition of the two phases given by the measurements of Blavette *et al.* [21, 22], the average scattering lengths of the two phases can be calculated ($\langle b_\gamma \rangle = 0.75 \times 10^{-12}\ \text{cm}$; $\langle b'_\gamma \rangle = 0.83 \times 10^{-12}\ \text{cm}$). Their difference is noticeable, so these superalloys produce an intense neutron scattering at small angles; measurements with good statistics can be obtained in less than 20 minutes.

Transmission Electron Microscopy (TEM) observations have been performed with a JEOL 200 CX apparatus on samples mechanically polished down to $80\ \mu\text{m}$ and electrothinned in a Milligan bath (10% HClO_4 , 90% 2-Butoxyethanol (Ethylene Glycol Monobutyl Ether)) with a voltage of 13.5 V. Then the samples were rinsed with Ethanol. The dark field technique has been used to reveal the precipitates. Scanning Electron Microscopy (SEM) observations of sample surfaces have been performed after chemical etching with a JEOL JSM 6400 apparatus.

3. Results.

3.1 TYPICAL SANS PATTERNS. — In figure 1 are presented typical iso-intensity contours of the SANS patterns obtained from AM1 samples corresponding to different thermomechanical histories. They illustrate the different types of results which can be obtained.

In (a), the sample was annealed during 2 hours at $1\,050\text{ }^\circ\text{C}$, the $\langle 001 \rangle$ axis was parallel to the direction of the incident neutron beam and the measurement was performed in the *small- q range*. The SANS pattern shows a characteristic fourfold symmetry indicating that both the shape and the arrangement of the precipitates evolve with a strong anisotropy along the crystallographic direction of the specimen. If the sample were not a single crystal, this information would disappear. Furthermore four peaks are observed along the $\langle 100 \rangle$ and $\langle 010 \rangle$ axes of the reciprocal lattice. These correlation peaks show that in the direct space, the precipitates are rather regularly arranged on the nodes of a simple cubic « superlattice » of

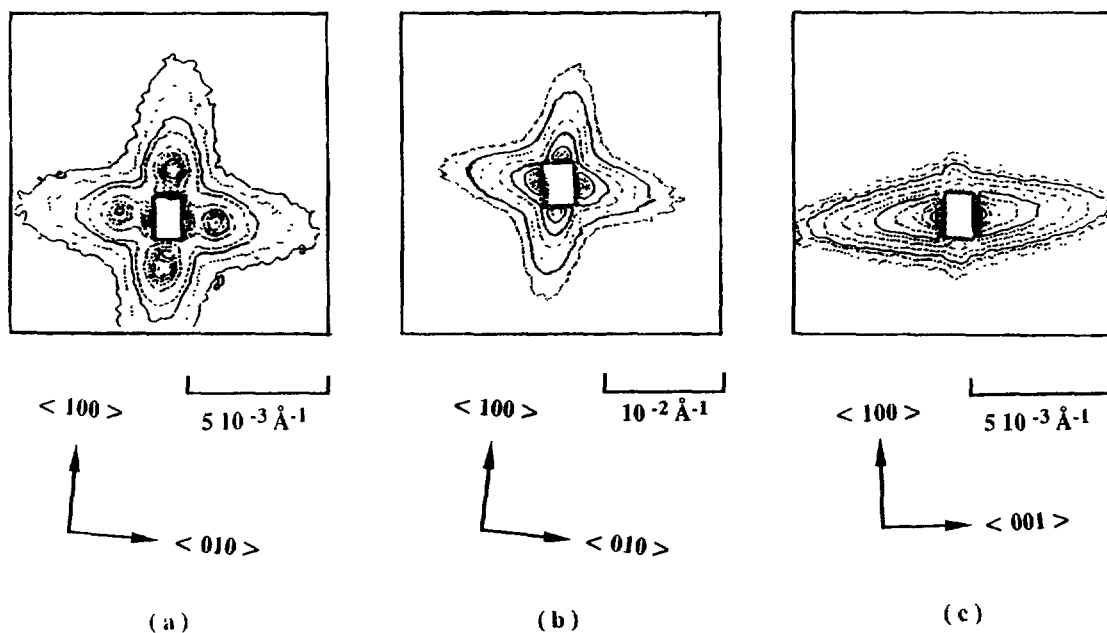


Fig. 1. — SANS iso-intensity contours obtained from AM1 superalloy samples with different thermo-mechanical history : a) annealed 2 hours at 1 050 °C, *small q range*, (001) plane, b) annealed 2 hours at 1 050 °C, *large q range*, (001) plane, c) crept at 950 °C, $\sigma = 280$ MPa, $\varepsilon = 1.5\%$ along the $\langle 001 \rangle$ direction, *small q range*, (010) plane.

parameter L , parallel to the crystallographic f.c.c. lattice. The parameter L is deduced from the position of the first correlation peaks because the higher order correlation peaks are not observed, indicating that translational order between the precipitates is only of short range.

In (b) the same sample is studied but in the *large-q range*. Far from the correlation peaks, one expects to observe mainly the Fourier transform of the average form factor of the individual precipitates and a fourfold symmetry is again observed according to a cuboidal shape of the precipitates. The single crystal character of the sample allows one to analyze the scattering in the observation plane as a function of the direction with respect to the crystallographic axes and also as a function of the orientation of the sample with respect to the incident neutron beam. Hence an anisotropic analysis of the average shape of the precipitates can be obtained as will be shown below.

In (c) the sample has been subjected to a classical ONERA heat treatment, and subsequently submitted to a creep test at SNECMA laboratories under the following conditions : $T = 950$ °C, tensile stress $\sigma = 280$ MPa, until a deformation of 1.5 % was obtained. With such a thermomechanical treatment, the γ' precipitates coarsen and become like platelets perpendicular to the $\langle 001 \rangle$ creep axis [6]. Figure 1c shows the SANS pattern obtained in the *small-q range* with the $\langle 001 \rangle$ axis perpendicular to the neutron direction. As expected a « cigar-shaped » scattering pattern is observed corresponding to the platelet-shape of the precipitates ; again the single crystal character of the sample allows one to observe this evolution. Due to the large size of the platelets, no correlation peak can be observed along the $\langle 100 \rangle$ axis which is parallel to their faces. However, along the $\langle 001 \rangle$ axis, the absence of correlation peak in the *small-q range* leads to assume that the interdistance between the platelets is broadly distributed.

As shown by these examples, the SANS technique appears well suited to the study of the γ' precipitates of superalloys and it has been used first to study the evolution of their morphology as a function of heat treatments.

3.2 INFLUENCE OF HEAT TREATMENTS ON THE MORPHOLOGY OF THE γ' PRECIPITATES.

3.2.1 Large- q range experiments.

3.2.1.1 Study on the (001) plane. — As stated above, in this q range, far from the correlation peaks, one expects to observe mainly the Fourier transform of the average form factor of the individual precipitates. Figure 2 shows the iso-intensity contours of the SANS patterns for samples annealed at 1 050 °C during 0 h, 2 h, 32 h and 480 h. A fourfold symmetry is observed for all the samples with slight deviations which are attributed to imperfect alignment of their $\langle 001 \rangle$ axis with respect to the incident beam. Nevertheless, for none of the samples, the cross-shape is well pronounced. This can be attributed to some orientational disorder or to a

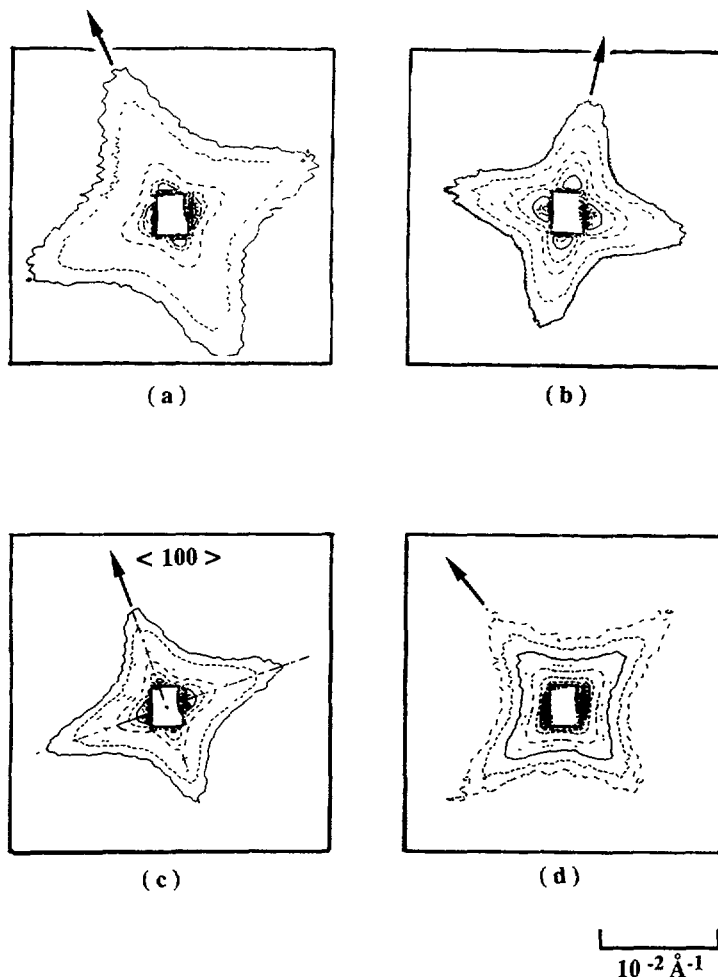


Fig. 2. — SANS iso-intensity contours in the (001) plane from AM1 superalloy samples for several annealing times at 1 050 °C: a) before annealing, b) annealed 2 hours, c) annealed 32 hours, d) annealed 480 hours. The arrows indicate the $\langle 100 \rangle$ directions.

curvature of the cubes' faces. Except a slight deformation of the SANS pattern in the first stage of annealing, there is no drastic modification of its shape with annealing time. In the q range of interest which is far from the correlation peaks, one studies the anisotropy of the asymptotic behaviour along the different axes. The asymptotic behaviour of the intensity scattered in $\langle 100 \rangle$ and $\langle 110 \rangle$ directions is plotted in figure 3 for two samples (annealed during 2 and 68 hours at $T = 1\,050\text{ }^\circ\text{C}$). The slopes of the curves $\text{Ln}(I)$ vs. $\text{Ln}(q)$ are close to

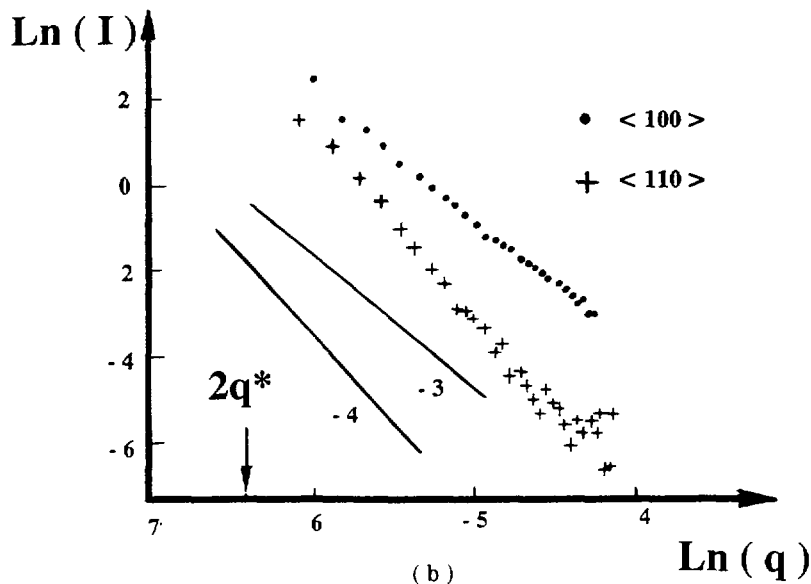
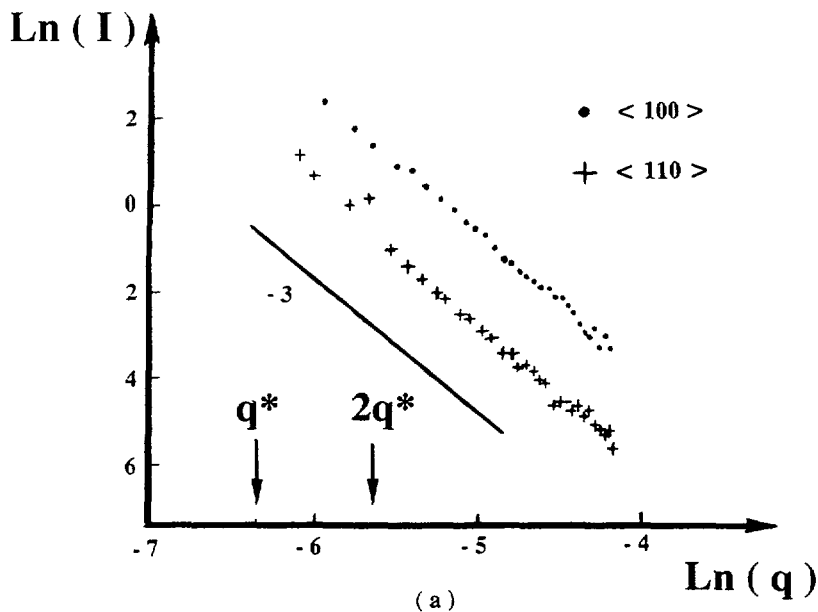


Fig. 3. — $\text{Ln}(I)$ versus $\text{Ln}(q)$ along the directions $\langle 100 \rangle$ and $\langle 110 \rangle$ for AM1 superalloy samples with different annealing times at $1\,050\text{ }^\circ\text{C}$: a) 2 hours, b) 68 hours. The slope corresponding to -3 and -4 are shown by continuous lines, q^* corresponds to the position of the correlation peak.

- 3 for the first sample in both directions, while for the sample annealed during 68 hours, they are close to - 3 and - 4 respectively for the $\langle 100 \rangle$ and $\langle 110 \rangle$ directions. These analyses provide more detailed information on the shape of precipitates, which will be discussed in the next section.

3.2.1.2 Changing the orientation of the sample with respect to the neutron beam. — In a next step, measurements were performed on the sample annealed during 128 hours at $T = 1\,050\text{ }^\circ\text{C}$ for different orientations of the sample rotated around the $\langle 100 \rangle$ crystallographic axis which was set vertical (and perpendicular to the incident neutron beam). Some SANS patterns are shown in figure 4 for several values of the ω angle, the value $\omega = 0$ corresponding to the neutron beam parallel to the $\langle 001 \rangle$ axis. So, close to this value, we found again the fourfold symmetry previously described. When ω is changed, the planes perpendicular to the rotation axis remain invariant, thus the two streaks along the $\langle 100 \rangle$ direction corresponding to these planes are always observed whereas the other streaks

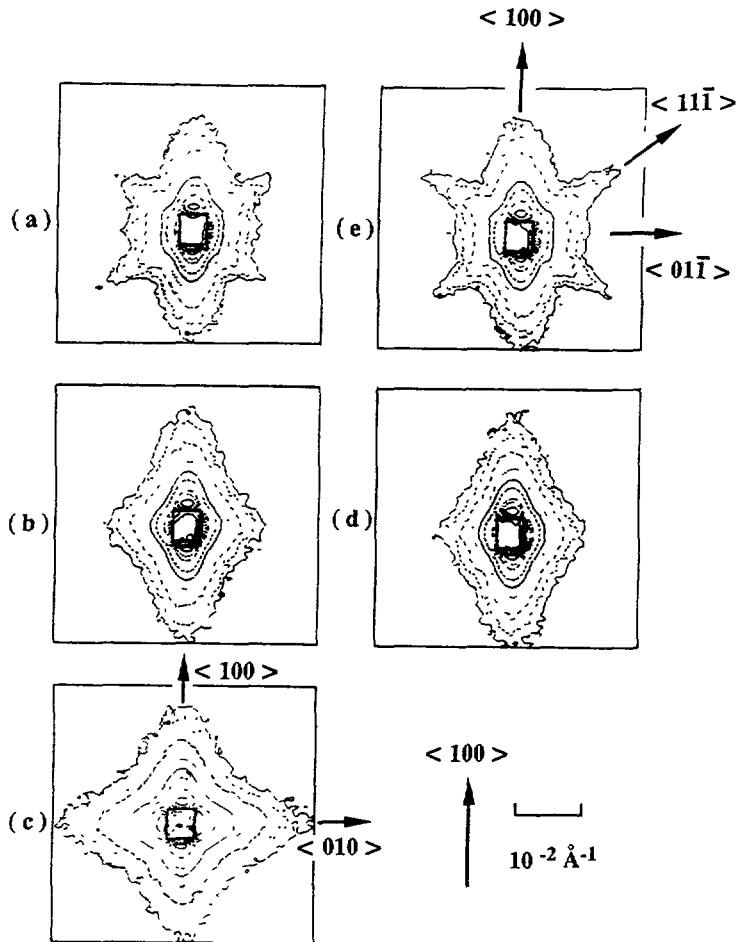


Fig. 4. — SANS iso-intensity contours of an AM1 superalloy sample annealed during 128 hours at $1\,050\text{ }^\circ\text{C}$, for different orientations ω of the crystal around the crystallographic axis $\langle 100 \rangle$: a) $\omega = -47.5^\circ$, b) $\omega = -27.5^\circ$, c) $\omega = 2.5^\circ$, d) $\omega = 32.5^\circ$, e) $\omega = 45^\circ$. For $\omega = 0$, the neutron beam is aligned to the $\langle 001 \rangle$ axis.

(previously parallel to the $\langle 010 \rangle$ disappear when the angle ω is different from 0° or 180°). The features described up to now are consistent with a cubic shape of the γ' precipitates. However, when the ω value is close to 45° , new streaks in the $\langle 111 \rangle$ type direction appear; they are observed within a very narrow ω range. These new streaks are only observed for large values of q ($q > 1.5 \times 10^{-2} \text{ \AA}^{-1}$). This means that the origin of these streaks corresponds to « small » distances in the direct space.

The same investigation has been performed on the sample annealed at $T = 1\,050^\circ\text{C}$ during 0.5 hour. In spite of a careful search, such streaks in the $\langle 111 \rangle$ directions have not been observed for this sample.

3.2.2 Small- q range observations in the (001) plane. — As shown in figure 1, in this q range, one can investigate « large » distances in the direct space, and correlation peaks corresponding to the rather regular arrangement of the precipitates are observed. Figure 5 shows the evolution of the SANS pattern as a function of the annealing time at $1\,050^\circ\text{C}$. It is clearly visible that the positions of the correlation peaks evolve towards smaller angles during annealing.

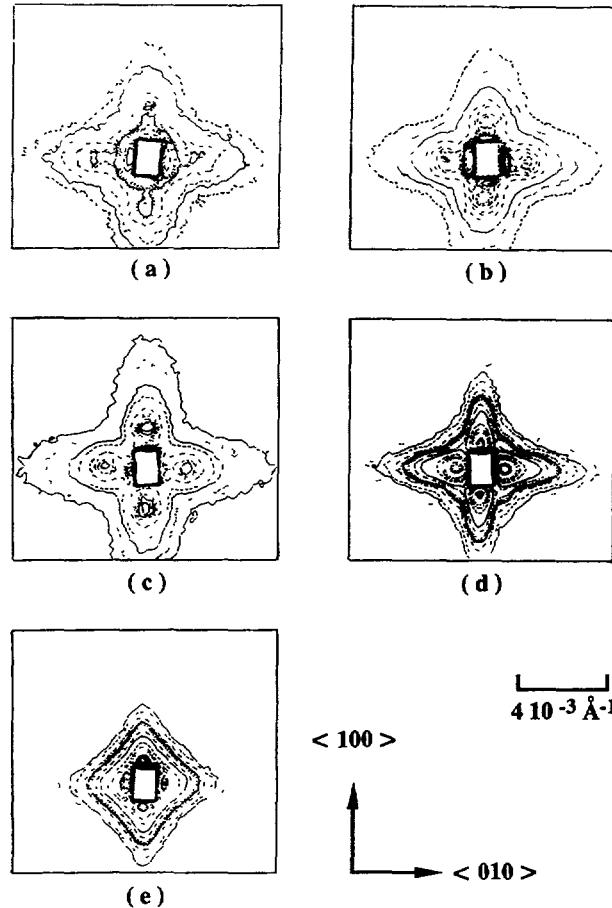


Fig. 5. — SANS iso-intensity contours in the (001) plane from AM1 superalloy single crystals for several annealing times at $1\,050^\circ\text{C}$: a) before annealing, b) annealed 0.5 hours, c) annealed 2 hours, d) annealed 32 hours, e) annealed 480 hours.

The intensity profiles along the $\langle 010 \rangle$ axes are plotted in figure 6 (linear scales). They have been obtained from the 2D patterns by integration over a strip of finite width ($\Delta q \approx 1.8 \times 10^{-4} \text{ \AA}^{-1}$) along the $\langle 100 \rangle$ direction. They clearly show the evolution of the correlation peaks with the duration of annealing.

Prior to annealing the specimen exhibits a very broad maximum around $q = 2 \times 10^{-3} \text{ \AA}^{-1}$ and at very small q ($q < 10^{-3} \text{ \AA}^{-1}$) the iso-intensity contours are circular i.e. the intensity scattered close to the origin is isotropic (Fig. 5a). So the expansion of the scattered intensity as a function of q limited to the second order terms, is valid in this q range where the intensity is insensitive to the cubic anisotropy. A detailed description of this behaviour would need to build a model which takes into account the cuboidal shape of the precipitates, their size and their interdistance, comparable to that developed by M. Hennion *et al.* [23] for ellipsoids. In a first approximation, although the system is not diluted, a Guinier plot of the intensity scattered in the small q range has been made and is shown in the insert of figure 6. It corresponds to the intensity scattered in the $\langle 110 \rangle$ direction along which no correlation peak is observed. The slope at small q allows us to estimate a radius of gyration $R_g = 0.1 \text{ \AA}$. This corresponds to a diameter $D = 0.26 \text{ \AA}$ for a spherical particle and to an edge $a = 0.2 \text{ \AA}$ for a cubic particle. These estimates are consistent with the value deduced from the position of the correlation peak (Tab. II). Let us stress however that the radius of gyration concept is only valid for dilute systems without interparticle interference. In the present case, these conditions are not fulfilled. In a densely packed system the contributions to the Guinier behaviour arise from the long-range behaviour of the correlation function. However from the observed behaviour of the scattered intensity around $q = 0$, we can conclude that the Guinier approach probes the same length scale as the analysis of the correlation peaks and that probably such an analysis would be well adapted to investigate earlier stages of the precipitation.

With increasing annealing times, the correlation peak becomes sharper corresponding to a better ordering of the γ' precipitates and shifts towards smaller q indicating an increase of their interdistance (coalescence). For annealing times larger than 32 hours, they move

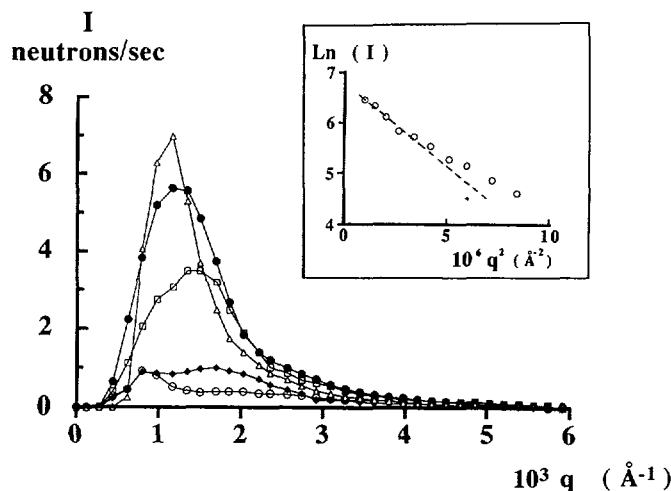


Fig. 6. — Intensity profiles along the $\langle 010 \rangle$ axis calculated from the iso-intensity contours for AM1 superalloy single crystals with different annealing times at 1 050 °C : (○) before annealing, (◆) annealed 2 hours, (□) annealed 8 hours, (●) annealed 16 hours, (△) annealed 32 hours. Insert : Guinier plot of the intensity along the $\langle 110 \rangle$ direction for the sample before annealing.

Table II. — Position of the correlation peak q^* and centre-to-centre spacing L between precipitates, for different annealing times t_a .

t_a (hours)	0	0.50	2	8	16	32
q^* ($10^{-3} \cdot \text{\AA}^{-1}$)	2.17	1.80	1.75	1.50	1.28	1.05
L (μm)	0.29	0.35	0.36	0.42	0.49	0.60

towards the beam stop and can no longer be observed. It may also be noted that in the *small q* range, the shape of the SANS iso-intensity contours evolves from a cross shape for intermediate heat treatments (2-32 hours) to a square shape for longer times (Fig. 5e).

4. Discussion.

SANS studies of the precipitation or coalescence of the γ' phase of superalloys have already been performed in polycrystalline samples [24, 25]. However the single crystal nature of our samples allows us to get more detailed information on the evolution of the shape and the size of the γ' precipitates.

4.1 SHAPE OF THE γ' PRECIPITATES. — Although the SANS patterns at large q (Fig. 2) have a fourfold symmetry, information concerning the shape of γ' precipitates is delicate to obtain because the interparticle interferences are mixed with the Fourier transform of individual particles. However, some information can be obtained from the asymptotic behaviour of the scattered intensity (i.e. when $\frac{q}{q^*} \approx \frac{qL}{2\pi} \gg 1$).

For a perfectly cubic precipitate with sharp edges, one expects the following behaviour :

- $I \sim q^{-2}$ along the $\langle 100 \rangle$ direction perpendicular to the cube faces
- $I \sim q^{-4}$ along any $\langle hk0 \rangle$ direction perpendicular to the edges
- $I \sim q^{-6}$ along any other $\langle hkl \rangle$ directions.

However, it is important to note that any distortion, even small, with respect to the perfect cube, induces another asymptotic behaviour which becomes relevant. Thus, the q^{-6} behaviour is unlikely to be observed ; for instance if the cubes are rounded, one must consider the asymptotic behaviour of curved interfaces i.e. :

- $I \sim q^{-4}$ along a normal to spherical surfaces
- $I \sim q^{-3}$ along a normal to cylindrical surfaces
- $I \sim q^{-2}$ along a normal to almost planar surfaces.

Furthermore, if there is an ensemble of precipitates with some orientational disorder, it is clear that the asymptotic behaviour $I \sim q^{-n}$ with the smallest exponent n , will extend farther than the others around the normal to the mean interface. This means that asymptotic behaviour is generally governed by the smaller n exponent.

The asymptotic behaviour in the $\langle 100 \rangle$ and $\langle 110 \rangle$ directions of a single crystal sample have been studied as a function of the annealing time (Fig. 3 shows two typical cases which have been observed). For short time of annealing (a few hours) the slopes of the double logarithmic

plots are approximately the same in both directions and their values are about -3 between $2q^*$ and $8q^*$. For large annealing times, the slope is about -3 along the $\langle 100 \rangle$ direction between $3q^*$ and $16q^*$ and -4 along the $\langle 110 \rangle$ direction in the same q range.

None of these kinds of asymptotic behaviour corresponds to perfect cubic shape of precipitates :

— for the sample annealed during 2 hours the q^{-3} behaviour in both directions would indicate cylindrical distortions of the faces and of the edges (but with different curvatures) ;

— for the sample annealed during 68 hours, there is almost no change for the intensity scattered normal to the faces but a q^{-4} dependence is observed along the normal to the edges. This may be interpreted either by the formation of sharper edges or by a double curvature of the edges. The latter assumption is consistent with the possible existence of truncated corners as discussed below from the streaks observed along the $\langle 111 \rangle$ directions.

The transmission electron microscopy (TEM) photographs of figure 7 confirm that the precipitate faces are not perfectly flat. Furthermore, it is observed that face orientations are slightly distributed with respect to the crystallographic axes. This may modify the asymptotic behaviour if the observed q range is not large enough. Some photographs also reveal the existence of very small γ' precipitates (a few hundred of Å) in the γ matrix. These precipitates are probably due to the small change of the volume fraction of the γ' phase between 1 050 °C and room temperature. However, they represent a very small volume of the sample and their contribution to the SANS pattern which occurs mainly at large q , is assumed to be negligible under the present experimental conditions.

The qualitative evolution of the SANS pattern for longer annealing times (Fig. 5e) can also be understood by the analysis of TEM photographs. Indeed, after the well known improvement of the cuboidal shape and of the regularity of the arrangement of the precipitates for annealing time of about 16 hours [5], the increase of the duration of the heat treatment leads to a departure from the cuboidal shape, with a more complicated concave shape resulting from the coalescence of two or three adjacent parallelepipeds.

We have also analysed the asymptotic behaviour of the streaks along the $\langle 111 \rangle$ direction (Fig. 4). Along this direction the slope is close to -2.7 and such a value is consistent with the existence of planes perpendicular to $\langle 111 \rangle$ type directions. Thus it seems reasonable to assume that the streaks are associated with a truncature of the cube corners. The high sensitivity of these streaks to the orientation of the sample is consistent with the alignment of the truncated corners along the $\langle 110 \rangle$ directions. In order to check this hypothesis we simulated the 2D Fourier transform of regular arrangements of rectangles with different types of corner truncatures. The diffusion patterns, in this 2D simulation, present streaks similar to those which have been observed when the truncatures are large enough. However in the 3D sample, the truncatures have not to be so large because they are aligned along the $\langle 110 \rangle$ axis and this may explain why they disappear when the incident beam is not parallel to a (111) plane. For a better understanding of this effect, it is of interest to consider, instead of the truncated cubes, the almost plate-like inter-precipitate γ regions perpendicular to the $\langle 111 \rangle$ directions. The fact that these streaks have been observed only for long annealing time (128 hours at $T = 1\ 050$ °C) shows that one of the effects produced by very long heat treatment is to erode the (111) corners, a feature which seems difficult to observe by electron microscopy technique but which can be important to understand the evolution of the precipitates. In the above discussion, we only analysed the symmetry and the asymptotic behaviour along a few crystallographic directions, while the SANS patterns of this single crystalline samples actually contain more information. A detailed study would require a complete set of orientations of the sample which could then be compared with results of 3D Fourier Transform simulations.

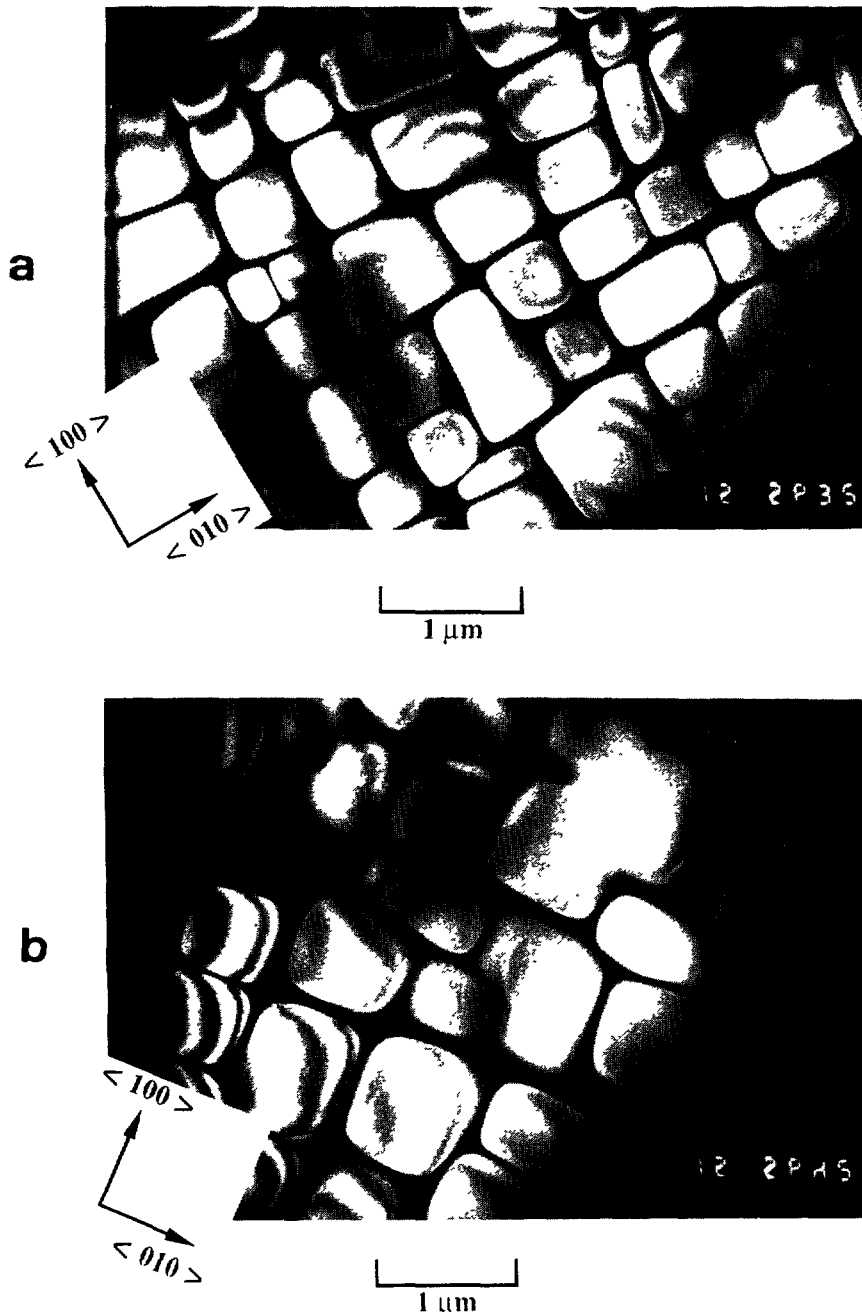


Fig. 7. — TEM observations of the γ' precipitates of the AM1 samples annealed at 1 050 °C during : a) 16 hours, b) 128 hours.

4.2 SIZE OF THE γ' PRECIPITATES. — When the correlation peaks are observed, i.e. when the size-distribution of the precipitates is not too broad, an approximate Bragg law can be applied to determine the average interdistance L between centres of mass of the γ' precipitates using : $q^* = \alpha 2 \pi/L$, where q^* is the scattering vector of the maximum of the intensity, and

α is a constant close to 1 which depends on the shape and on the size distribution of the precipitates [25]. Due to the coarsening of the precipitates and taking into account the limited resolution of the instrument, correlation peaks were only observed for annealing times up to 32 hours at 1 050 °C. In this range, q^* and L were determined (assuming $\alpha = 1$) and the results are reported in table II. In order to check the validity of this determination, some samples were also studied by scanning electron microscopy (SEM). Figure 8 shows a photograph obtained on the sample annealed during 2 hours. From the number of precipitates on the photograph, their average interdistance was estimated to be between 0.35 μm and 0.40 μm depending on the considered region of the sample surface, in good agreement with the SANS determination (Tab. II). However it is important to note that :

i) the value obtained by SANS corresponds to an average over about 10^{11} precipitates, in the bulk specimen, while those obtained by SEM are averaged over less than 10^3 precipitates at the surface of the specimen ;

ii) As the distribution of size is rather broad, the value obtained by SANS may be slightly overestimated due to a larger contribution of the large precipitates, and to the assumption that : $\alpha = 1$.

iii) The agreement between values of obtained from both techniques becomes worse for long annealing times (up to 30 % of difference) but in this case the number of precipitates observed by SEM is small and the inhomogeneous coarsening in the specimen due, for instance, to the dendritic structure has to be taken into account [26].

From electron microscopy observations, it can be noted that the precipitates have rather the shape of parallelepipeds ; the cubic shape being only an « average » model shape as

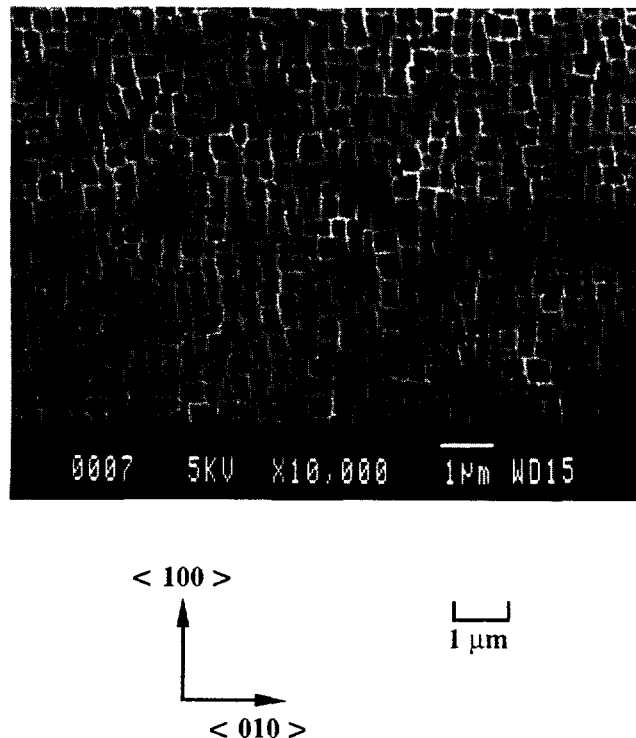


Fig. 8. — SEM observation of the γ' precipitates of the AM1 superalloy sample annealed during 2 hours at 1 050 °C.

previously reported by Caron *et al.* [5]. Therefore the position of the precipitates on the nodes of a cubic « superlattice » is only an average arrangement with no long-range order. This is probably one of the causes of the absence of second-order correlation peaks.

In figure 9, the average volume of the precipitates L^3 has been plotted *versus* the annealing time t_a : it increases proportionally with the duration of the annealing except for short annealing times. As in the present case, it is assumed that at room temperature the volume fraction of the γ' phase does not depend on the previous heat treatments, one can conclude that the growth of the precipitates is controlled by a mechanism of coalescence. The results, shown in figure 9, are consistent with the usual coalescence theory of Lifshitz, Slyosov and Wagner [27]. This means that simple diffusion is not the only mechanism limiting the growth of the precipitates; there are also topological constraints which can induce the « collapse » of small precipitates into larger ones, as shown by the results of TEM. Let us also remark that $L^3(\sim t_a)$ represents the average volume of the precipitates under the assumption that the growth of the precipitates is the same along the three cubic axes.

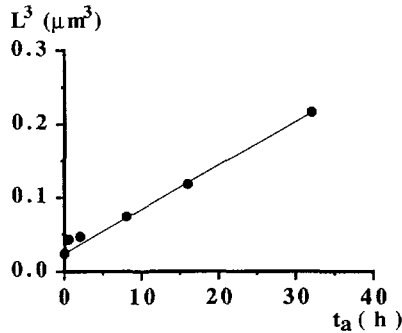


Fig. 9. — Evolution of the average volume of the γ' precipitates *versus* annealing time t_a at 1 050 °C.

From a technological point of view the $t_a^{1/3}$ dependence of L can be used to predict the size of γ' precipitates after heat treatment, a parameter which is of particular importance for the mechanical properties of these alloys.

5. Conclusion.

As shown by this study, the single crystal character of the samples permits detailed information to be extracted from SANS investigation. The scattering patterns recorded for different orientations of the specimens provide information on the evolution of the average shape of the precipitates during coarsening. In particular starting from a rather spherical shape in a cubic arrangement, the precipitates become cubic shaped but the asymptotic behaviour indicates that the edges are not sharp and that the faces are not flat. Possible truncatures of their corners are suggested after a long annealing. Also the centre-to-centre spacing between the precipitates which is determined from the correlation peak, has the advantage to be averaged on a large number of precipitates eliminating the possible effects due to inhomogeneities in the sample.

It is important to note that experiments can be performed in an oven, allowing « *in situ* » measurements during the thermal treatments [18]. As the scattering is rather intense (an exploitable SANS pattern can be obtained in less than 5 minutes), the study of the kinetics of the coalescence (for which the main evolution occurs during a few hours) or of the

precipitation is now possible on the same sample without necessity of quenching different specimens.

As shown by the observation performed on the crept sample, the SANS technique also permits us to study the oriented coalescence of the γ' precipitates on these single crystalline samples. This study can be made on quenched samples but the possibility to perform « *in situ* » experiment would allow us to observe the early stage of the « rafting ». This would permit a better understanding of the mechanisms and of the kinetic of this transformation which is also very important for the mechanical properties of these alloys.

Acknowledgments.

This work has been supported by the « Groupement Scientifique » of CNRS « Microstructure et propriétés des superalliages monocristallins ». Samples were provided by SNECMA which is gratefully acknowledged for its interest in this work.

We wish to express our thanks to C. Pratt for spark cutting the AM1 single crystals, and to G. Commandeur for the sample preparation. We are grateful to J. Garden for his help during scanning electron microscopy observations.

Experiments were performed at the « Institut Laue Langevin » at Grenoble. We are grateful to the Institut for the allocation of facilities. We acknowledge its staff and particularly R. Ghosh and A. Rennie for their help.

References

- [1] EZZ S. S., POPE D. P., PAIDAR V., *Acta Metall.* **30** (1982) 921.
- [2] HERTEMAN J. P., *Mat. Techn.* **10** (1985) 559.
- [3] REPPICH B., SCHEPP P., WEHNER G., *Acta Metall.* **30** (1982) 95.
- [4] CHUNG D. W., CHATWEDI M., LLOYD D. J., *Acta Metall.* **24** (1976) 227.
- [5] CARON P., KHAN T., *Mat. Sci. Eng.* **61** (1983) 173.
- [6] KHAN T., CARON P., FOURNIER D., HARRIS K., *Mat. Techn.* **10-11** (1985) 567.
- [7] NATHAL M. V. *Met. Trans.* **18A** (1987) 1961.
- [8] MACKAY R. A., NATHAL M. V., *Acta Metall.* **38** (1990) 993.
- [9] FREDHOLM A., Thèse de Doctorat (Ecole Nationale Supérieure des Mines de Paris), (1987).
- [10] BONNET R., ATI A., *J. Microsc. Spectrosc. Electron* **14** (1989) 169.
- [11] BERTRAND C., DALLAS J. P., RZEPSKI J., SIDHOM N., TRICHET M. F., CORNET M., Mémoires et Etudes Scientifiques Revue de Métallurgie (juin 1989) p. 333.
- [12] NATHAL M. V., MACKAY R. A., GARLICK R. G., *Mat. Sci. Eng.* **75** (1985) 195.
- [13] BELLET D., BASTIE P., *Philos. Mag.* **B 64** (1991) 143.
- [14] Brevet Français N° 2 557 598, SNECMA, Imphy, Armines, ONERA (1983).
- [15] GUINIER A., FOURNET G., « Small Angle Scattering of X-Rays » (Wiley, New York, 1955).
- [16] FEIGIN L. A., SVERGUN D. I., Structure Analysis by Small Angle X-Ray and neutron Scattering (Plenum Press, New York and London, 1987).
- [17] BRASS A. M., CHÈNE J., SERVANT C., Mémoires et Etudes Scientifiques, *Rev. Metall.* (sept. 1989) p. 526.
- [18] I.L.L., Annual Experimental Report (1989) p. 367, (1990) p. 336 and cover sheet.
- [19] IBEL K., *J. Appl. Cryst.* **9** (1976) 296.
- [20] Guide to Neutron Research Facilities at the I.L.L. (Yellow Book, 1988) p. 28.
- [21] BLAVETTE D., BOSTEL A., *Acta Metall.* **32** (1984) 811.

- [22] BUCHON A., CHAMBRELAND S., BLAVETTE D., Comptes Rendus du Colloque « Superalliages Monocristallins » (Nancy 1990) p. 129.
- [23] HENNION M., RONZAUD D., GUYOT P., *Acta Metall.* **30** (1982) 599.
- [24] SCHWAHN D., KESTERNICH W., SCHUSTER H., *Met. trans.* **12A** (1981) 155.
- [25] MESSOLORAS S., STEWART R. J., *J. Appl. Cryst.* **21** (1988) 870.
- [26] HAZOTTE A., LACAZE J., *Scripta Met.* **23** (1989) 1877.
- [27] LIFSHITZ I. M., SLYOSOV V. V., *J. Phys. Chem. Solids* **19** (1961) 35.